Received: 2 December 2022 | Revised: 20 June 2023 | Accepted: 24 July 2023

DOI: 10.1111/ejn.16116

SPECIAL ISSUE ARTICLE

EJN European Journal of Neuroscience FENS WILEY

Single closed-loop acoustic stimulation targeting memory consolidation suppressed hippocampal ripple and thalamo-cortical spindle activity in mice

Sonat Aksamaz[1,2] | Matthias Mölle[2,3] | Esther Olubukola Akinola[1,2] | Erik Gromodka[1] | Maxim Bazhenov[4] | Lisa Marshall[1,2,3]

[1]Institute of Experimental and Clinical Pharmacology, University of Lübeck, Lübeck, Germany

[2]University Medical Center Schleswig-Holstein, Lübeck, Germany

[3]Center of Brain, Behavior and Metabolism, Lübeck, Germany

[4]Department of Medicine, University of California San Diego, La Jolla, CA, USA

Correspondence
Lisa Marshall, Institute of Experimental and Clinical Pharmacology, University of Lübeck. Lübeck, Germany.
Email: lisa.marshall@pharma.uni-luebeck.de;
lisa.marshall@uni-luebeck.de

Funding information
National Science Foundation/ Bundesministerium für Bildung und Forschung, Grant/Award Numbers: 01GQ1706, IIS-1724405, EFRI BRAID: 2223839; National Institutes of Health, Grant/Award Numbers: 1RO1MH125557, 1R01NS109553, 1RO1MH117155, 1R01NS104368

Edited by: Antoine Adamantidis

Abstract

Brain rhythms of sleep reflect neuronal activity underlying sleep-associated memory consolidation. The modulation of brain rhythms, such as the sleep slow oscillation (SO), is used both to investigate neurophysiological mechanisms as well as to measure the impact of sleep on presumed functional correlates. Previously, closed-loop acoustic stimulation in humans targeted to the SO Up-state successfully enhanced the slow oscillation rhythm and phase-dependent spindle activity, although effects on memory retention have varied. Here, we aim to disclose relations between stimulation-induced hippocampo-thalamo-cortical activity and retention performance on a hippocampus-dependent object-place recognition task in mice by applying acoustic stimulation at four estimated SO phases compared to sham condition. Across the 3-h retention interval at the beginning of the light phase closed-loop stimulation failed to improve retention significantly over sham. However, retention during SO Up-state stimulation was significantly higher than for another SO phase. At all SO phases, acoustic stimulation was accompanied by a sharp increase in ripple activity followed by about a second-long suppression of hippocampal sharp wave ripple and longer maintained suppression of thalamo-cortical spindle activity. Importantly, dynamics of SO-coupled hippocampal ripple activity distinguished SOUp-state stimulation. Non-rapid eye movement (NREM) sleep was not impacted by stimulation, yet preREM sleep duration was effected. Results reveal the complex effect of stimulation on the brain dynamics and support the use of closed-loop acoustic stimulation in mice to investigate the inter-regional mechanisms underlying memory consolidation.

Abbreviations: CG, Cingulate Gyrus; CLAS, Closed-loop acoustic stimulation; DHC, Dorsal hippocampus; EEG, Electroencephalogram; EMG, Electromyography; FIR, Finite impulse response; LFP, Local field potential; NREM, Non-rapid eye movement; OPR, Object place recognition; preREM, Pre rapid eye movement; PVC, Polyvinyl chloride; REM, Rapid eye movement; RMS, Root mean square; s.c., Subcutaneous; sCLAS, Single closed-loop acoustic stimulation; SO, Slow Oscillation; SPWRs, Sharp wave ripples.

KEYWORDS
non-invasive brain stimulation, sharp wave ripples, sleep, slow oscillation, spatial memory

1 | INTRODUCTION

According to the concept of active systems consolidation, long-term memory formation involving hippocampus-dependent episodic memory rests on the active transfer of information from hippocampal neural representations to the neocortex, after an initial neocortical tagging or engram formation (Tonegawa et al., 2018). This transfer involves reactivation processes through which representations are integrated into distributed neural networks (Klinzing et al., 2019; Marshall et al., 2020; Oudiette et al., 2013; Rasch & Born, 2013). Hippocampal activity associated with sharp wave ripples (SPWRS) was first suggested to underlie information transfer from hippocampus to neocortex (Buzsáki, 1989). Since then hippocampal SPWRs, thalamo-cortical sleep spindles, cortical slow oscillations of NREM sleep and their temporal interplay are strongly associated with memory consolidation processes, as discussed in multiple reviews (Adamantidis et al., 2019; Diekelmann & Born, 2010; Girardeau & Lopes-Dos-Santos, 2021; Rasch & Born, 2013). Supportive interrogation studies in rodents have shown that the suppression of hippocampal ripples is detrimental for memory consolidation (Ego-Stengel & Wilson, 2010; Girardeau et al., 2009), similar to reduced spindle-ripple coupling as a result of targeted disruption of spindle activity (Novitskaya et al., 2016; Swift et al., 2018). Moreover, enhanced coupling between SPWR and slow waves induced by electric stimulation facilitated memory consolidation (Maingret et al., 2016).

In humans multiple studies have employed non-invasive brain stimulation procedures to investigate relations between brain rhythms and memory function, and to probe for future clinical applications (Ketz et al., 2018; Ladenbauer et al., 2021; Marshall et al., 2006; Ngo, Martinetz, et al., 2013; Salfi et al., 2020). Non-invasive brain stimulation presents a procedure to interact mildly with the brain's neural activity. Thus, in particular, acoustic and electric stimuli are used experimentally to probe the brains responsiveness, and thus disclose features of endogenous neural activity and their functional correlates (Campos-Beltran & Marshall, 2017; Girardeau & Lopes-Dos-Santos, 2021; Malkani & Zee, 2020). In the closed-loop acoustic stimulation (CLAS) procedure in humans a pair of short (50 ms) stimuli are delivered during non-rapid eye movement (NREM) sleep, with both stimuli arriving approximately during the SO Up-state (Ngo, Martinetz, et al., 2013). In this first seminal paper hippocampus-dependent memory consolidation was enhanced by CLAS as compared to a sham session. Although CLAS during NREM sleep appears on average to modulate endogenous EEG SO and spindle activity in a robust fashion (Koo-Poeggel et al., 2022; Moreira et al., 2021; Ngo, Martinetz, et al., 2013; Ong et al., 2016), effects on memory consolidation were found to be weak and less conclusive as concluded from a recent meta-analyses (Wunderlin et al., 2021). Moreover, hippocampal responses to CLAS during hippocampus-dependent memory-consolidation remain undisclosed. Only one magnetic resonance study reported increased task-dependent hippocampal activity after a session of CLAS as compared to a sham session (Ong et al., 2020).

The aim of the current study was therefore to investigate the thalamo-cortical and hippocampal interactions induced by CLAS during NREM sleep, together with the effect on retention performance. Since responses of the auditory system reveal stimulus and species specific-differences, even amongst rodents (Cromwell et al., 2008; Ngo et al., 2015; Ngo, Claussen, et al., 2013; Süer et al., 2004; Witten et al., 2016), the present study investigated electrophysiological and behavioural response only to a single acoustic stimulus delivered in a closed loop fashion. To distinguish this stimulation from the initial CLAS protocol by Ngo and colleagues with two closely successive stimuli (Ngo, Martinetz, et al., 2013), we use the term single CLAS (sCLAS) here. Retention performance was assessed on the hippocampus-dependent object place recognition (OPR) task (Barker & Warburton, 2011; Mumby et al., 2002). We found that sCLAS delivered during NREM sleep indeed modified retention performance in an SO-phase-dependent manner. Furthermore, the study revealed a sharp increase in hippocampal ripple activity and subsequently pronounced suppression of both thalamo-cortical spindle and hippocampal SPWR activity in the range of seconds post-stimulation. Our results suggest that sCLAS can actively modify NREM sleep-dependent consolidation but further studies are needed to reveal optimal and possibly individualized stimulation protocols to increase memory performance.

2 | MATERIALS AND METHODS

2.1 | Animals

Subjects were male C5BL/6 N mice (Janvier, France), 8–10 weeks on arrival. Due to technical reasons only

10 mice entered the study. Surgery was performed between 10 and 12 weeks of age. Housing was in Type II-Long IVC cages (Greenline, Tecniplast, GM500) on a 12 h light/dark cycle (lights on: 7:00 h or 8:00 h) with ad libitum access to food and water; initially with littermates and individually after electrode implantation. Animals were handled for 5 min per day for 5 days before the surgery. All animals were treated identically, and all procedures were concordant with the European and national guidelines (EU Directive 2010/63/EU) and were approved by the local state authority (Ministerium für Energiewende, Landwirtschaft, Umwelt und ländliche Räume, Schleswig-Holstein).

2.2 | Electrode implantation

Isoflurane (induction: 3.5%, maintenance 0.8–2% at 1–1.3 L/min O_2) was used to anaesthetize the animals. They were placed into a stereotactic frame (David Kopf Instruments). To ease the breathing 0.04 mg/kg atropine (Atropinum Sulfuricum, Eifelfango) was administered subcutaneously (s.c.). After shaving and disinfection of the area, lidocaine (1% solution, B. Braun Melsungen) was injected s.c. before any scalp incision. Every 30 min of surgery 0.1 ml of warm saline was injected s.c. to substitute fluid loss. An array of five tungsten wires (40 µm, California Fine Wire) was implanted into cingulate gyrus, CG (AP: 1.2, L: 0.3, DV: −0.75) and another array of five tungsten wires, cut slightly diagonally, was implanted into the dorsal hippocampus, dHC (AP: -1.94, L: 1.5, DV; deepest wire: −1.35) for recording LFP activity (Figure 1a). Two stainless-steel screws (Bilaney, Germany) were used as reference and ground electrodes, implanted above the cerebellum (AP: −4.80, L: 0.00) and the somatosensory cortex (AP: −2, L: 2), respectively. A polyimide-insulated stainless-steel wire (0.125 mm diameter, Plastics One) inserted into the neck muscles was used for recording EMG. Wire ends of all electrodes were soldered to a plug-connector during surgery and secured with dental acrylic (Super-Bond, Sun Medical or Relyx Unicem 2 Automix, 3 M; Grip Cement, 3 M; and Palapress, Heraeus Kulzer). Finally, the head stage was encircled by copper wire mesh. Before discontinuing the isoflurane supply carprofen (5 mg/kg, Rimadyl, Pfizer) was given intraperitoneal for pain relief. To substitute for fluid loss at the end of the surgery 0.5 ml of warm saline were given s.c. Animals were kept under red light in their home cage until they became mobile and were then transferred back to the animal holding room where they spent at least 7 days for recovery.

2.3 | General procedure

After recovery from surgery in the animal holding room mice were subjected to two habituations sessions for tethering and time in the sleep box (see **Apparatuses and objects** and **Habituation to the recording procedure**) and thereafter three OPR-habituation sessions (see **Habituation to the object place recognition task**) which all took place in the experimental room. In the experiment proper each of the five OPR sessions consisted of a sample phase, a retention and test phase (see **Object place recognition task**; Figure 1b). The sample phase began within the first hour after lights on. It was followed by a 3-hour retention interval during which electrophysiology was recorded (see **Electrophysiological data acquisition**), after which the OPR test phase was performed. Mice were subsequently returned to their home cage and taken to the animal holding room. The study had a within-subject design with the five OPR sessions presenting the repeated measures. Sessions were separated each by 5–8 days to prevent interference from previous short-term memories.

Mice participated in five OPR sessions corresponding to the four delays between detection of the SO trough and delivery of a trigger for stimulation, and a sham session. In the four delay conditions targeting different SO phases (2 ms, 120 ms, 180 ms or 300 ms, see **single closed-loop acoustic stimulation;** Figure 1c,d), every other acoustic stimulation was followed by a (silent) pseudo-stimulation. The order of sessions was pseudo-randomized, so that across animals the delays occurred in different orders.

2.4 | Apparatuses and objects

The experimental apparatus for the object place recognition task was a dark grey open-field box (37 cm wide× 37 cm deep × 35 cm high, Ewald Kongsbak GmbH + Co. KG) made of polyvinyl chloride (PVC). For all experiments, the light intensity was set to 100 lx above the open field. A webcam (Logitech HD webcam, model C310), was mounted above the open-field. Extramaze cues were represented by the camera stand. Objects were glass bottles of various shapes, textures, and size (height 11–20 cm, bottom diameter 5–6 cm), each type was filled with sand of a different colour. They had sufficient weight to ensure the mice could not displace them. Before each sample and test phase, as well as after each session objects and open fields were cleaned thoroughly with 70% ethanol solution to remove any residual scents. For electrophysiological recording, a smaller dark grey box was used (20 cm × 20 cm × 31 cm, dark grey PVC; Fachhochschule Lübeck PROJEKT, Germany).

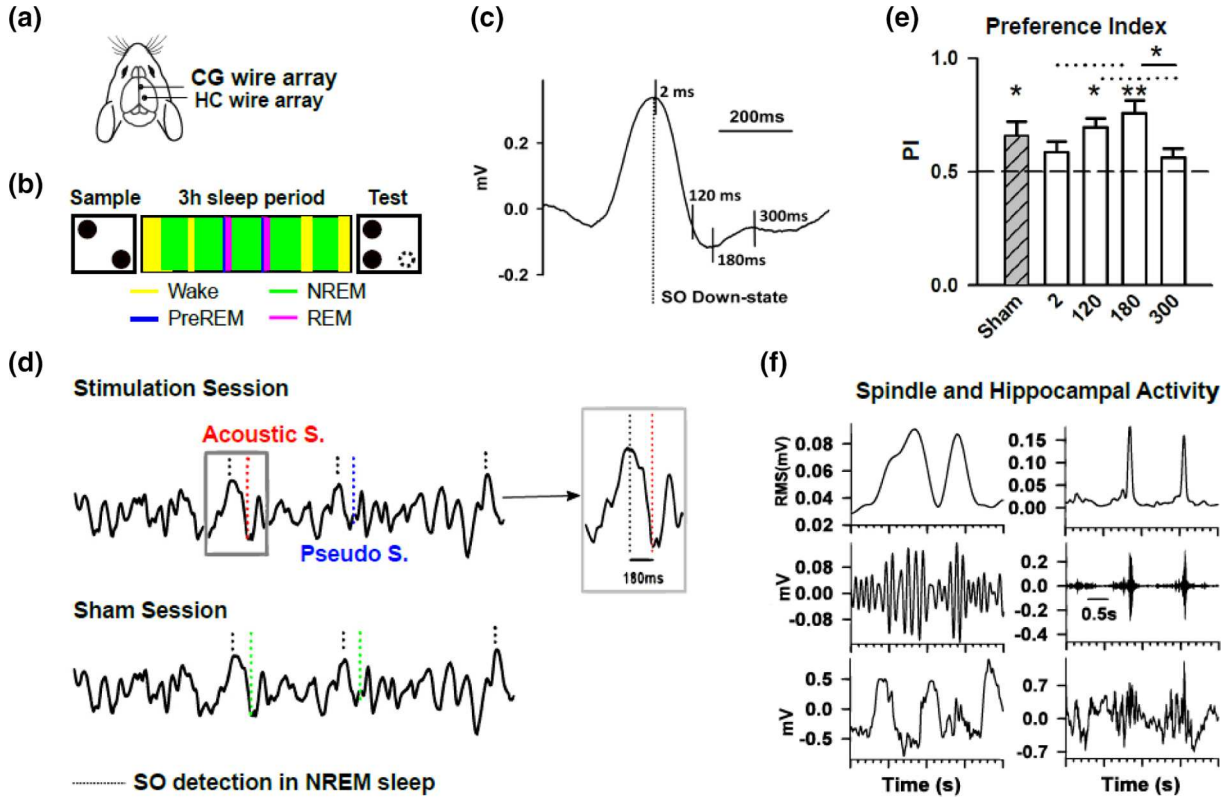

FIGURE 1 **Visualization of electrode positions, experimental design, sCLAS application, and behavioural results. a.** Positions of cortical and dorsal hippocampal wire array electrodes on the mouse brain. **b.** Time frame of one OPR session: following lights on, animals were placed in the open field for 10 min to perform the sample phase of the OPR test. Thereafter animals were tethered to the amplifier and allowed to sleep for 3 hours in the recording box. After the sleep period, animals were untethered and transferred to the open field for the OPR test phase (5 min). **c.** A schematic of the four delays relative to SO Down-state peak. **d.** Schematic of SO detection and sCLAS application for the same LFP deflections in a stimulation session with 180 ms delay and a sham session. Black dotted lines indicate SO detection. Corresponding time points for the 180 ms delay of sham are indicated by black and green dotted lines. In the stimulation session, SO detection is followed alternately by an acoustic stimulation and a pseudo-stimulation. The sham session remained completely without an acoustic stimulation. The minimal inter-stimulus interval is always 2.5 s. **e.** Mean (± SEM) preference for the replaced object across all conditions. Deviation from the chance level (PI = 0.5) is represented by asterisks above the bars. White bars represent the four delay conditions included in the ANOVA to investigate SO phase dependence. Corresponding post-hoc ANOVA results are indicated by the asterisk ($p \leq 0.05$) and the horizontal dotted lines ($p \leq 0.10$). Ten animals participated in the study, however in two conditions due to data loss numbers are reduced (120 ms, n = 7; 300 ms, n = 6). **f.** For spindle (left) and SPWR (right) an example of the raw LFP signal (bottom), filtered LFP (middle) and RMS signals (top) as used for further analyses.

2.5 | Habituation to the recording procedure

Mice spent the end of the last light phase and consecutive dark phase in the recording box, untethered. After lights were on, mice were connected to the head stage and electrophysiological activity was monitored for 3 h. Thereafter mice were returned to the holding room. Habituation recordings took place on two consecutive days and the data from the second day was analyzed to determine the cortical SO threshold and hippocampal delta/theta ratio for the sCLAS in the experiments proper.

2.6 | Habituation to the object place recognition task

After one hour in the experimental room mice were put into a clean transfer cage, then placed into the middle of the open field and allowed to explore for 10 minutes. Thereafter mice were returned to the holding room. This procedure took place on three consecutive days.

2.7 | Object place recognition task

The mean age of the animals on the first day of the OPR was 97.90 ± 6.15 days. Shortly before lights out animals

were taken from their holding to the experimental room. In the experimental room, the OPR sample phase started on average 39.2 ± 2.0 min and electrophysiological recording 55.4 ± 2.1 min after lights on. In brief, in the OPR sample phase (10 min) mice were exposed to two identical objects, which were placed in two corners of the field. Special care was taken that animals were exposed to the same texture on the objects (e.g., any 3D imprint would either always face the animal or the wall). Between sample and test phases lay a 3 h retention interval during which time animals were tethered to the recording amplifier for electrophysiological recording. For the test phase (5 min) one of the objects had been displaced to one of the other two free corners whereas the other object remained at its position. Positioning of the displaced object was pseudo-randomized. After the OPR task animals were returned to the holding room.

2.8 | Electrophysiological data acquisition

For electrophysiological recordings, the electrode connector was attached to a head-stage microamplifier (μPA16, Multi Channel Systems MCS GmbH, Germany). Electrophysiological signals were amplified (amplifier gain: 400) and digitally sampled with 4 kHz through a portable ME16 System (ME16-FAI-μPA, Multi Channel Systems MCS GmbH, Germany) and stored on an assigned computer (MC_Rack software, Multi Channel Systems MCS GmbH, Germany). Animals had ad libitum access to food and water in the recording box.

Real-time analogue signals from one CG and one dHC LFP wire electrode were transferred through two audio outputs of the ME16 System to the data acquisition interface CED Power1401-3 (Cambridge Electronic Design Limited, Cambridge, England) which was connected to a second computer. The CED 1401-3, its application program Spike 2 and a custom-made program based on the built-in script language were used for continuous online calculation of hippocampal delta/theta ratios and for cortical SO detection.

2.9 | Determination of SO-threshold and delta/theta ratio for the single acoustic closed-loop stimulation during NREM sleep

For each individual animal, hippocampal data from the second habituation recording were used for offline determination of the most suitable delta/theta ratio threshold, which was then used in the experimental recording sessions for online NREM sleep detection. Furthermore, data from a CG signal were used to determine the initial threshold for the online SO detection. The threshold of hippocampal delta/theta ratio was calculated and finally set by visual inspection from two histograms showing the distribution of all delta/theta ratio values of all sleep stages, one histogram for NREM sleep and another histogram for Wake and REM sleep see **Supplementary Figure S1**). Analyses to determine the SO detection threshold were limited to NREM sleep epochs, and the same algorithm was applied for offline threshold detections. This algorithm is described in detail further below.

2.10 | Single closed-loop acoustic stimulation

As long as the delta/theta ratio was above the threshold for NREM sleep, if the SO detection threshold, indicating a Down-state, was surpassed by the CG LFP deflection, an acoustic or pseudo-stimulation was delivered and a trigger, of a corresponding code, generated. A trigger devoid of stimulation (pseudo-stimulation) was generated for every other detected SO; i.e. acoustic and pseudo-stimulation alternated. Following SO detection and corresponding stimulation, the algorithm was paused automatically for 2.5 s. In addition, the SO-detection algorithm could be manually paused by the experimenter, e.g. during long periods of movement. For acoustic stimulation an analog signal, consisting of 10 ms acoustic white noise, was sent from the Power1401-3 to two dome tweeters (TW 6 NG 8 Ω, Visaton, Germany) inside of the recording box through a custom-made stereo audio amplifier (2 × 5 W) at 58 dBA volume, producing simultaneous acoustic stimulation.

Online detection of SOs was conducted by a custom-made script running under Spike 2 software together with a sequencer in the Power1401-3, like that described in Ngo, Martinetz, et al. (2013). In brief, each time the LFP signal crossed an adaptive threshold toward larger (positive) values, an acoustic or pseudo-stimulation was triggered. On default, the threshold was set to the initial value calculated from the second habituation recording. Every 0.5 s, the threshold was updated to the maximal (i.e., largest positive) instantaneous amplitude of the CG signal within the preceding 2 s interval, however, only if this value exceeded the initial threshold. This algorithm ensured a continuously reliable detection of gradually increasing and decreasing SO amplitude during sleep or within a sleep cycle by its positive half-wave peak (Down-state peak).

The timing of all SO detections was marked digitally (with different numbers for acoustic stimulation and pseudo-stimulation) in the Spike 2 data file and these markers were also transferred to the ME16 System to be

saved with the MC_Rack Software along with the animal's cortical and hippocampal data on a separate channel. The delay between the SO detection and the delivery of the acoustic or pseudo-stimulation differed between each stimulation condition: 2 ms, 120 ms, 180 ms, and 300 ms, corresponding on average to the SO Down-state, Down-to-Up-state transition, Up-state and Up-to-Down-state transition/late Up-state, respectively. In the sham condition, as also for pseudo-stimulation of the delay conditions, all triggers were devoid of acoustic stimulation.

2.11 | Data analysis

2.11.1 | Object place recognition task

Spatial retention performance was measured as the preference index, calculated as the ratio of exploration time of the displaced object to the total exploration time of both objects during the test phase. Thus, a preference index differing significantly from chance level (0.5) indicates maintained object memory (Dere et al., 2007). Exploratory behaviour was assessed by manual scoring of behavioural videos by an experimenter blind to the experimental condition and previous placement of the objects using a tracking software (AnyMaze, Stoelting, version 4.72). The time spent by mice actively exploring each object was rated manually. Mice were considered exploring an object when they faced and touched the object with its nose and/or forepaws. Grooming, freezing behaviour in close vicinity to objects, and closely passing the object or touching it with the tail or body were not scored as exploration.

2.11.2 | Sleep architecture

An experimental rater assigned sleep stages to all 5 s epochs of the 3 h sleep recording according to the standard criteria using the CG and dHC LFP signals as well as EMG recordings (SleepSign for Animals, Kissei Comtec). Briefly, the sleep stages were characterized as follows: wakefulness (Wake) by high EMG activity and desynchronized CG LFP; NREM sleep by low EMG and high-amplitude low-frequency CG LFP activity consisting mostly of delta activity (0.75–4 Hz); pre-rapid eye movement sleep (PreREM) by low EMG and high-amplitude CG sigma (10–15 Hz) activity before REM sleep or Wake; and REM sleep by low EMG activity and high theta activity (6–10 Hz) in the HC LFP.

Furthermore, after scoring the 3 h sleep period, NREM sleep was divided into two equal-length periods, without splitting sleep cycles, termed 'early' and 'late' NREM sleep, to compare selected effects.

2.11.3 | Electrophysiology

Electrophysiological analyses were conducted on the LFP recording from the NREM sleep epochs over the 3 h post-learning period or within early and late NREM sleep periods. LFP data included one chosen CG and HC channel from each animal. Data were analyzed using Spike2 (Cambridge Electronic Design) and custom scripts written with the built-in script language.

2.11.4 | Offline event detection

SO, spindle and ripple events were identified similar to Binder et al. (2019). In brief, to identify SOs in the CG LFP signal, a low-pass finite impulse response (FIR) filter of 30 Hz was applied and the resultant signal was down-sampled to 100 Hz. Subsequently, a low-pass FIR filter of 3.5 Hz was used to produce the SO signal. In the slow oscillation signal, all two succeeding negative-to-positive zero crossings separated by 0.45–1.43 s (corresponding to 0.7–2.22 Hz) were marked and the negative and the positive peak potentials between these marked negative-to-positive zero crossings were registered. SO events were defined as those intervals that displayed (1) a positive peak amplitude of 1.25 times the average positive peak amplitude of this animals sham session or higher (2) a positive-to-negative peak amplitude difference of at least 1.25 times the average positive-to-negative peak amplitude difference of the respective sham session. To calculate event-event correlations offline detected SOs were divided into two groups: (1) those SOs for which an online stimulation occurred in the interval of ± 1.5 seconds around the SO downstate peak value (acoustic-ON) and (2) SOs for which no online stimulation occurred in the corresponding interval (acoustic-OFF).

Spindle identification also required first low-pass (<30 Hz) filtering and down-sampling to 100 Hz of the CG LFP. Subsequently, a FIR bandpass filter of 9–15 Hz was applied and a root mean square (RMS) representation of the filtered signal was generated by using a 0.2 s long sliding window. The resulting RMS signal was smoothed additionally with a sliding window average of 0.2 s. Time frames were considered as spindle intervals if the RMS signal exceeded a threshold of 1.25 SD of the bandpass-filtered signal for 0.5–3 s and if the largest value within the frame was >2 SD of the bandpass filtered signal. For each animal individual thresholds were calculated from the bandpass filtered signal of the sham

session. Two succeeding spindles were counted as one spindle when the interval between the end of the first spindle and the beginning of the second spindle was shorter than 0.5 s and the resulting (merged) spindle was not >3 s. Detected events were not accepted as spindles when the difference between the largest and smallest potential of the low-pass filtered signal (<30 Hz) within the frame was 5 times larger than 2 SD of the bandpass filtered signal and the time between these two extrema was equal or shorter than one-half of an oscillation cycle of 15 Hz (0.033 s). For event-correlation analyses, the peaks and troughs of every detected spindle were marked as the maxima and minima of the bandpass filtered signal (between the beginning and end of the spindle), and the deepest trough was designated as the "spindle peak" that represented the respective spindle in time, i.e., the time point taken for referencing event correlation histograms (see description of event correlation histograms later in this section).

Identification of ripples initially required the application of a low-pass FIR filter of 300 Hz and downsampling to 1 kHz of the dorsal hippocampal LFP. Subsequently, a bandpass FIR filter of 150–200 Hz was applied and the RMS signal was calculated with a sliding 0.02 s time window. The RMS signal was then smoothed with a sliding window average of 0.02 s. Time frames were considered as ripple intervals if the RMS signal exceeded a threshold of 1.25 SD of the bandpass-filtered signal for 0.025–0.1 s and if the largest value within the frame was >5 SD of the bandpass-filtered signal. For each animal, individual thresholds were calculated from the bandpass-filtered signal of the sham session. Detected events were not accepted as ripples when the difference between the largest and smallest potential of the low-pass filtered signal (<300 Hz) within the frame was 5 times larger than 5 SD of the bandpass filtered signal and the time between these two extrema was equal or shorter than one-half of an oscillation cycle of 200 Hz (2.5 ms). For event-correlation analyses, the peaks and troughs of every ripple were marked as the maxima and minima of the bandpass-filtered signal, and the deepest trough was designated as the "ripple peak" that represented the respective ripple in time.

Durations of SO, spindle and SPWR oscillatory events correspond to the time from beginning to end of the detected oscillatory event, respectively. Density values refer to the mean density of the corresponding event across all NREM sleep epochs. SO, spindle and ripple amplitudes are defined as the mean peak-to-peak values of events detected from the corresponding filtered frequency band signal. Spindle and ripple RMS represent the average values across all detected oscillatory events. The SO slope was derived from the positive Down-state peak to the following zero crossing of the SO-filtered signal. Corresponding grand mean averages of the detected SOs, spindles, and ripples across all animals were calculated for the different conditions. Also, averages of the original signal, spindle RMS and ripple RMS were calculated for acoustic stimulation of all delays and corresponding pseudo-stimulation.

2.11.5 | Stimulus-event correlation histograms

Stimulus-event correlation histograms were calculated for SO (Down-state peaks), spindle and ripple activity (number of peaks and troughs) in intervals of −1.0 to 2.5 s around the online detected and stimulated SOs. These histograms, with a bin size of 50 ms, were separately calculated for all acoustic- and all pseudo-stimulations during NREM sleep over the entire 3 h recording session. The individual histograms were z-scored by the corresponding mean and SD of the SO, spindle and ripple activity, respectively, for each animal during the −1.0 to 2.5 s interval to eliminate the considerable variability across animals and conditions, and for each animal subsequently baseline normalized (−1.0 to −0.5 ms). These histograms represent the acute modulatory effect of sCLAS on event activity. Grand mean averages of the stimulus-event correlation histograms across all animals were calculated for the different conditions and per-condition differences between acoustic- and all pseudo-stimulation were statistically tested.

2.11.6 | Event-event correlation histograms

Event-event correlation histograms were calculated for spindle and ripple activity (number of peaks and troughs) with reference to the time of the SO positive Down-state peak as identified in the CG LFP signal, separately for SOs for which a stimulation occurred (in the interval of ± 1.5 s around the SO downstate) and SOs for which no stimulation occurred. Additionally, event-event correlation histograms were calculated for spindle activity (number of peaks and troughs) with reference to the time of the ripple peak and for ripple activity (number of peaks and troughs) with reference to the time of the spindle peak. For all event-event correlation histograms, 3 s windows were used with an offset of 1.5 s and a bin size of 50 ms. Again, these histograms were calculated for all NREM sleep epochs over the entire 3 h recording session and additionally for early and late NREM sleep. The individual histograms were z-scored by the corresponding mean and SD of the spindle and ripple activity,

respectively, for each animal during the ±1.5 s interval to eliminate the considerable variability across animals and conditions, and for each animal subsequently, baseline normalized (−1.0 to −0.7 ms). The histograms represent a measure for the probability of activity of one event at a given time to proceed or follow another event, i.e., for the coupling of SOs, cortical spindles and hippocampal ripples.

2.12 | Statistical analysis

The study was conducted as a within-subject design, with five sessions. For statistical analyses of the preference index, the mean score of each session was first compared to the odds ratio of 0.5 by a one-sample t-test. Behavioural data were then subjected to a mixed-effects model for repeated measures analyses of variance (ANOVA) and posthoc paired t-tests.

Duration of sleep stages; and number of stimulation triggers given at a certain sleep stage for the 3 h interval, and event parameters of SOs, spindles, and SPWRs were subjected to mixed effects models for repeated measures with the factors Condition (Sham, 2 ms, 120 ms, 180 ms, 300 ms delay). Correction for multiple comparisons was conducted using the Holm-Sidak method (software package Prism 8, GraphPad Software, Inc.). Statistical comparisons of event-related activity, stimulus-event histograms of acoustic and pseudo-stimulation, and event-event correlation histograms were conducted by running (paired) t-tests and the Benjamini–Hochberg procedure was applied to control the false discovery rate (FDR; Benjamini & Hochberg, 1995). All data are expressed as mean ± SEM. A p-value < 0.05 was considered significant.

3 | RESULTS

FIGURE 1 (A-C) gives an overview of the recording locations (A), the OPR task with an exemplary distribution of sleep stages (B), a schematic of the four delays for acoustic stimulation and approximate SO phase: 2 ms (SO Down-state), 120 ms (Down-to-Up-state transition), 180 ms (Up-state) and 300 ms (Up-to-Down-state transition/late Up-state) (C), and schematics of stimulation and sham sessions (D).

3.1 | Effect of sCLAS on behaviour

Figure 1e shows the deviation of the preference index from chance level (corresponding to 50% preference for the displaced object) for the four delay conditions and sham. Of the four sCLAS delays an above chance performance was only obtained for the 120 and 180 ms delay condition (one sample t-test; theoretical mean: 0.5, sham: $t(9) = 2.525$, $p = 0.033$; 2 ms, $t(9) = 1.784$, $p = 0.1081$; 120 ms: $t(6) = 5.039$, $p = 0.024$; 180 ms: $t(9) = 4.613$, $p = 0.001$; 300 ms, $t(5) = 1.375$, $p = 0.2275$). For the 180 ms (Up-state) and 120 ms (Down-to-Up-state-transition) delays mice performed above chance level, but this was also true for sham. Thus, the effect of sCLAS across all conditions only revealed a trend (mixed-effects model; $F\ [4, 38] = 2.105$, $p = 0.099$). However, a mixed effects ANOVA model exclusively for the four conditions proved a modulation of behaviour dependent upon the phase of SO stimulation ($F[3,29] = 3.366$, $p = 0.032$). On this basis, we conducted post-hoc tests for the preference index between the four delay conditions. Here, results support increased retention performance for sCLAS at the 180 ms Up-state, but also a tendency toward increased performance for the preceding Down-to-Up-state transition at 120 ms as compared to either the Down-state or Up-to-Down-state transition/late Up-state (180 ms vs. 300 ms: $t\ (5) = 3.362$, $p = 0.020$; 180 vs. 2 ms: $t\ (9) = 2.164$, $p = 0.059$; 120 vs. 300 ms: $t\ (5) = 2.113$, $p = 0.088$). An exploratory test between the preference indexes at 180 ms delay and sham was not significant ($t(9) = 1.251$, $p = 0.243$, Figure 1e).

In summary, sCLAS modified memory retention dependent upon SO phase but was not successful in increasing performance significantly above sham.

3.2 | sCLAS application did not disrupt NREM sleep

To control whether sCLAS may have modified sleep composition, we investigated the proportion of sleep stages within the 3 h post-learning interval across differential stimulation conditions (Table 1). Only the duration of PreREM sleep revealed an effect of Condition ($F\ [4, 29] = 2.911$, $p = 0.038$). Pre-REM sleep is a transitional stage between NREM and REM sleep characterized by high-amplitude cortical spindles and low-frequency hippocampal theta activity (Glin et al., 1991). PreREM sleep duration in the condition with 180 ms delay was longer than that at 300 ms (mean difference 2.46 ± 0.80 min, $p = 0.044$, post-hoc Holm-Sidak multiple comparison test). No other sleep stage differed in duration between conditions).

Across all conditions, a mean number per session of 531.06 ± 21.91 acoustic or pseudo-stimulations, respectively, were delivered. There was no difference in the number of stimuli delivered between conditions within

TABLE 1 sCLAS did not disrupt NREM sleep.

		NREM (%)		PreREM (%)		REM (%)		Wake (%)	
Sham		50.94 ± 2.23		6.24 ± 0.71		2.22 ± 0.67		40.6 ± 2.94	
2 ms		51.47 ± 3.89		6.09 ± 0.69		1.9 ± 0.48		40.53 ± 4.32	
120 ms		55.3 ± 3.3		7.51 ± 1.04		2.11 ± 0.54		34.87 ± 2.95	
180 ms		53.8 ± 1.4		7.51 ± 0.64*		2.49 ± 0.44		36.22 ± 1.76	
300 ms		50.91 ± 2.9		5.81 ± 0.93*		1.85 ± 0.34		37.8 ± 1.77	
	F	***p***	***F***	***p***	***F***	***p***	***F***	***p***
Condition (4,29)	0.432	0.784	2.911	0.038	1.054	0.396	0.710	0.591

any of the sleep stages ($F(4,28) < 1.242$, $p > 0.316$ (in the sham session triggers of one animal could not be retrieved, thus reducing the statistical degrees of freedom as compared to Table 1). The percentage of stimuli given in the different sleep stages was as 80.09 ± 2.3% (NREM sleep), 0.53 ± 0.15% (PreREM sleep), 2.01 ± 0.13% (REM sleep) and 15.71 ± 1.41% (wake). The unexpected large number of stimulations during wakefulness for all conditions is most likely due to a poor online distinction between NREM sleep and quiet wakefulness in some animals in which EMG recording quality did not permit optimal assessment of muscle tone.

In summary, sCLAS only influenced time spent in preREM sleep that was manifested in a longer preREM sleep duration for stimulation at the 180 ms delay as compared to the 300 ms delay.

Table 1. Distribution of sleep stages during the 3 h recording interval in percent. Total sleep time was on average 186.06 ± 1.03 min. * $p < 0.05$, for the difference between the 180 ms and 300 ms sessions for PreREM sleep duration, post-hoc Holm-Sidak multiple comparison test. F and p values of mixed effects models are given. Number of animals in each group: 2 ms, 180 ms, n = 10; 120 ms, n = 7; 300 ms; n = 6; sham, n = 9. In the sham session triggers of one animal could not be retrieved. Mean ± SEM.

3.3 | sCLAS did not affect parameters of classical NREM sleep events

Following the affirmation that NREM sleep duration was preserved across the different sCLAS conditions, sleep-event parameters relevant to memory retention were analyzed. Neither density, amplitude nor duration of SOs, spindles nor SPWRs revealed any significant Condition effect (each $p \geq 0.1$, mixed-effects analyses; **Supplementary Table S1**; for detailed analyses see **Supplementary Tables S2-S4 and Figure S2**). Only spindle duration came close to a trend ($F[4,27] = 2.136$, $p = 0.104$). Since the duration of PreREM sleep, during which spindle-like activity occurs, differed between 300 and 180 ms, we specifically compared corresponding spindle durations. These analyses revealed longer mean spindle duration at the 180 ms than 300 ms delay condition by 48 ± 18 ms ($t(5) = 2.585$, $p = 0.049$, uncorrected for multiple comparisons).

Neither SO slope, nor spindle nor ripple RMS revealed a significant effect of Condition (each $p \geq 0.1$, mixed-effects analyses). Values presented in Table 2 are thus mean values collapsed across all conditions. In summary, at most spindle duration was affected by delay condition of sCLAS.

Table 2. Event parameters of density, amplitude, duration, and slope or RMS, respectively were analyzed for SO, spindle and SPWR events within NREM sleep of the 3 h post-learning interval. Mean ± SEM are given for all groups independent of the condition. SO and ripple parameters, n = 43; spindle parameters, n = 41. Spindle density values of one animal were spuriously high, thus data on this animal were omitted.

3.4 | Event-related activity

Here we analyzed the temporal relationship of evoked cortical local field potentials, thalamo-cortical spindle and hippocampal ripple root mean square values (RMS). Calculations of the latter are schematized in Figure 1f. For the four sCLAS conditions, **Figure 2** depicts the event-related responses to the acoustic stimuli and pseudo-stimulation. During the delay conditions, acoustic and pseudo-stimulation occurred alternately, with the trigger for pseudo-stimulation based on the identical criteria as for the acoustic stimulation of sCLAS. Event-related LFPs at the cingulate cortex confirm that stimulation adequately targeted the four different SO phases (**Figure 2a,b**, top rows). Interestingly, relative to the preceding baseline a significant enhancement of relatively long-lasting positive values, (i.e., values of the same

TABLE 2 Average sleep-event parameters across sCLAS conditions.

Event	Density (min^{-1})	Amplitude (mV)	Duration (ms)	RMS (μV)	Slope (mV/s)
SO	12.32 ± 0.69	0.62 ± 0.03	703 ± 4.14	-	0.83 ± 0.04
Spindle	2.36 ± 0.15	0.40 ± 0.011	843 ± 13.5	93 ± 2.55	-
SWPR	15.60 ± 1.13	0.18 ± 0.010	70 ± 0.75	39 ± 2.19	-

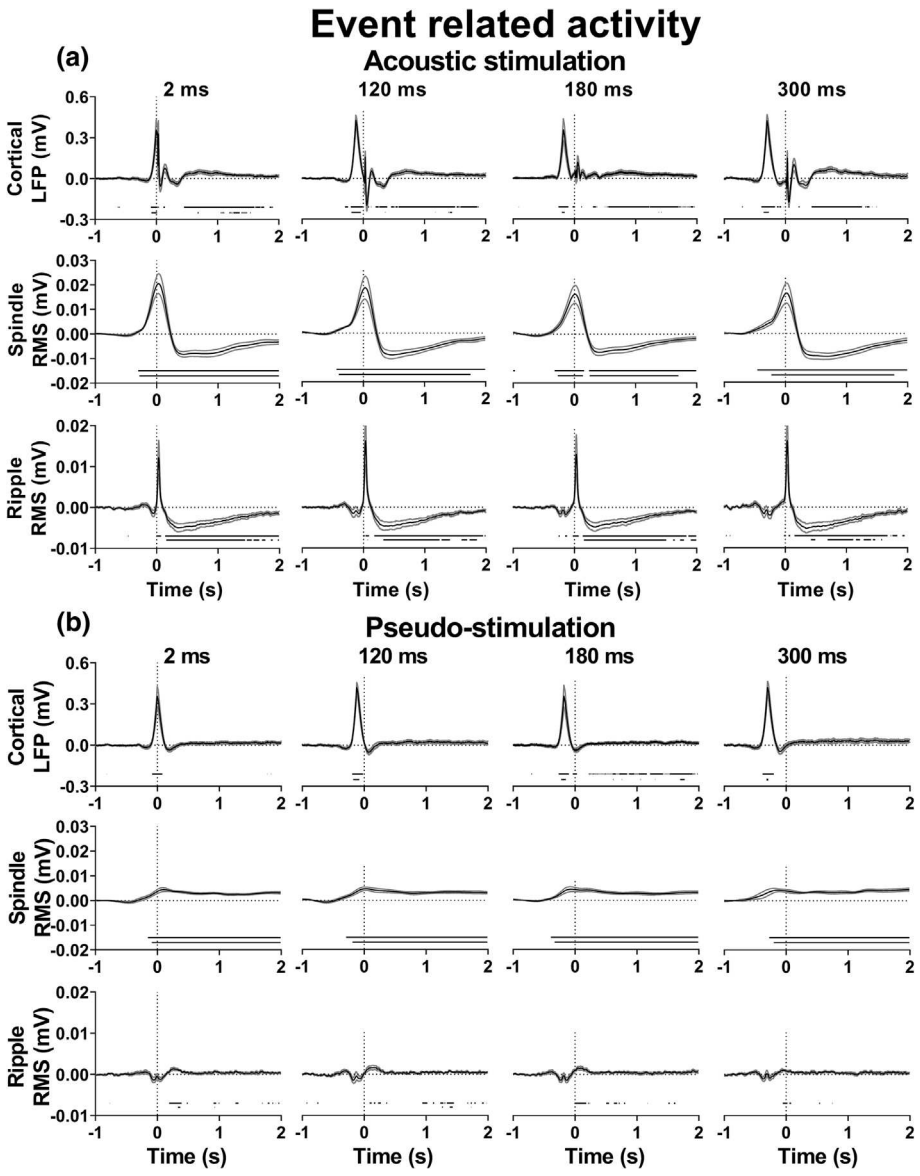

FIGURE 2 **sCLAS delivery time-locked to the differential SO-phases modulates cortical local field potential (LFP), cortical spindle and hippocampal ripple activity**. **a.** Acoustic stimulation. **b.** Pseudo-stimulation. **a, b.** From top to bottom, baseline normalized mean (± SEM) cortical LFP, spindle RMS, and CA1 SPWRs RMS. Horizontal lines correspond to significant differences from the baseline level (−1 to −0.5 s; paired t-tests) for false discovery rates set to 0.05 (top line) and 0.01 (bottom line). T = 0 s corresponds to the time of stimulation. 2 ms, 180 ms, n = 10; 120 ms, n = 7; 300 ms, n = 6.

polarity as the SO Down-state) only appeared for pseudo-stimulation at 180 ms, i.e., following acoustic Up-state stimulation (**Figure 2b** top row). Spindle RMS of pseudo-stimulation reveals for all conditions the typical increase commencing at the transition from the hyperpolarizing Down- to the depolarizing SO Up-state. Endogenous hippocampal ripple RMS commenced significantly with the emerging SO Up-state (**Figure 2b**).

For all conditions, the most consistent result of acoustic sCLAS in the cortical LFP signals was a 1 to 2 sec sustained increase of the positive potentials (**Figure 2a**, top), that had for pseudo-stimulation only obtained significance after the 180 ms delay (**Figure 2b**, top). Spindle and ripple RMS after acoustic stimulation differ greatly from pseudo-stimulation by revealing a significantly sustained suppression after a sharp increment in ripple RMS, and a broad enhancement in spindle RMS (**Figure 2a**). To determine whether hippocampal SPWRs were not merely a reflection of cortical activity in the ripple frequency range, the cortical LFP signal was analyzed

in the ripple frequency range (**Figure 3**). Cortical RMS in the ripple frequency range was also significantly modulation by the acoustic sCLAS, but overall of lower magnitude than hippocampal ripple RMS.

3.5 | Sustained suppression of spindle and ripple event activity following sCLAS

The prior section indicates for spindle and ripple RMS different temporal dynamics of acoustic and pseudo-stimulation, as compared to their respective baseline (**Figure 2**). Next, we compared SO, spindle and SPWR event activity directly between acoustic and pseudo-stimulation, i.e., within the same delay condition (Figure 4, **Supplementary Figure S3**). Expectedly, SO event activity was enhanced for both acoustic and pseudo-stimulation around $t = 0$ s, i.e., around the detected SO Down-state peak (SO trough). Most pronounced, again, was the significant suppression of both spindle and ripple event correlations, for acoustic compared to pseudo-stimulus event correlations (Figure 4b,c; **Supplementary Figure S3**). SPWR stimulus-event correlations increased sharply with acoustic as compared to pseudo-stimulation on average, significance was however limited, most likely due to a high temporal jitter of the short-lasting stimulus events between animals.

Together, acoustic vs. pseudo-stimulation led to a pronounced attenuation of both spindle and SPWR event activity. The steep mean enhancement in ripple event activity with acoustic stimulation did not reach significance for all SO phases.

3.6 | Is retention performance reflected by enhanced coupling to SO activity?

A prominent role of SOs in promoting memory consolidation is to group other sleep events. Therefore, we investigated if sCLAS application at the different SO phases affected the coupling of thalamo-cortical spindle and hippocampal ripple activities to SOs. Here offline detected SOs of NREM sleep were analyzed throughout the entire 3 h sleep interval. Since stimulus-induced responses did not occur during all epochs surrounding an offline detected SO, we distinguished between acoustic-ON and OFF epochs (cp. Methods). Only ON epochs containing offline detected SO together with an acoustic stimulation are presented in Figure 5 for the 2 and 180 ms delay conditions (**Supplementary Figure S4** for delay conditions 120 and 300 ms).

All event-event correlation histograms of sham reflect the characteristic temporal relationships between the neural oscillations: SO-spindle event-event correlations are minimal around the SO Down-state (SO trough) and increase with the Down-to-Up-state transition (sham in Figure 5a,b, left). Similarly, SO-ripple event-event correlations are minimal shortly prior to the SO Down-state, increasing at the Down-to-Up- state transition and peak around the Up-state (sham in Figure 5a,b, right). During the 3 h retention interval of both Down- and Up-state sCLAS conditions spindles are less modulated by the SO than in sham. Prior to the SO trough event-event correlations are significantly increased for acoustic-ON as compared to sham, and post SO trough correlations are significantly decreased. The latter most likely reflects the suppressed spindle activity after the acoustic stimulus (cp. also **Supplementary Figure S4**). Within a short time window at or after the offline detected SO the behaviour of coupled ripple events deviated from sham, yet in different ways. In the 2 ms delay, Down-state stimulation condition acoustic-ON SO-ripple event-event correlations were significantly fewer at the Down- to Up-state transition compared to sham. For Up-state stimulation (180 ms) acoustic-ON SO-ripple event-event correlations were not significantly fewer until endogenous SO-ripple coupling began to decrease, analogous to a facilitated coupling decrement.

Finally, the comparison of acoustic-ON SO-ripple event correlations between the 2 and 180 ms delay conditions (Figure 5c, right) revealed significantly more

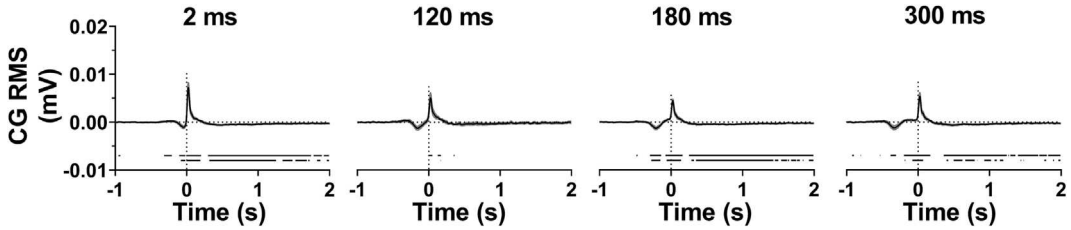

FIGURE 3 **sCLAS delivery time-locked to the differential SO-phases modulates cortical activity in the ripple frequency band.** For acoustic stimulation, baseline normalized (mean ± SEM) cortical RMS for the four delay conditions. Horizontal lines correspond to significant differences from the baseline level (−1 to −0.5 s, paired t-tests) for false discovery rate set to 0.05 (top line) and 0.01 (bottom line). T = 0 s corresponds to the time of stimulation. 2 ms, 180 ms, n = 10; 120 ms, n = 7; 300 ms, n = 6.

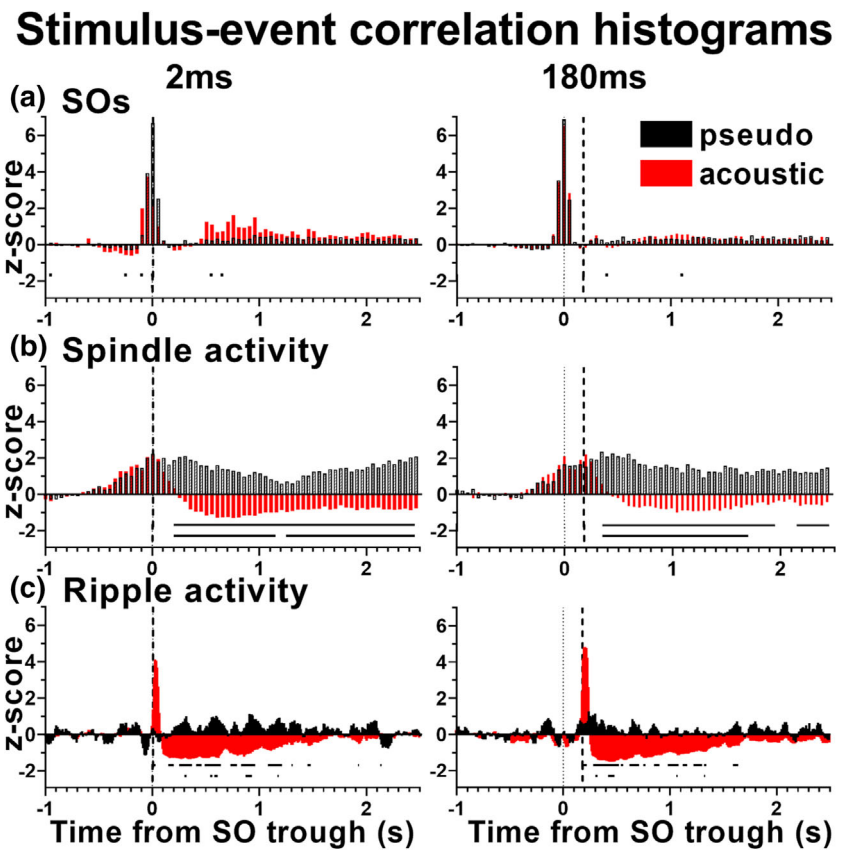

FIGURE 4 **SO, thalamo-cortical spindle and hippocampal ripple event-activity relative to sCLAS. a-c.** mean stimulus-event correlations for SO, spindle and CA1 SPWR events (z-transformed and baseline normalized, −1 to −0.5 s) for acoustic and pseudo-stimulation averaged across the 3 h interval for the 2 ms and 180 ms delay conditions, respectively. T = 0 s corresponds to the detected SO Down-state peak. Horizontal lines correspond to significant differences between acoustic and pseudo-stimulation (paired t-tests) for false discovery rates set to 0.05 (top line) and 0.01 (bottom line). Results are presented for the two delay conditions with a behavioural preference index significantly above (180 ms) and not significantly different from the chance level (2 ms), and for which data from all ten animals are available. Comparable figures for the other two delay conditions are given in the **supplementary Figure S3**.

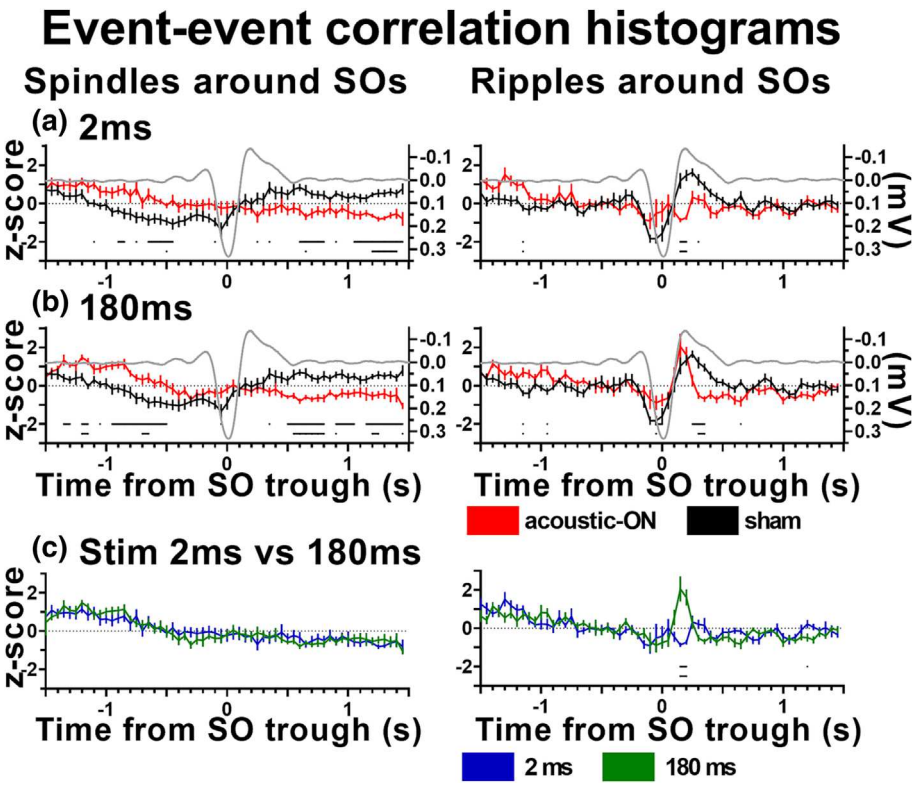

FIGURE 5 **Event-event coupling histograms between SO, spindle and SPWR event activity, respectively. a.** SO-spindle event-event (left) and SO-SPWR event-event correlations (right) time-locked to the positive Down-state peak of the SO (t = 0, SO trough) for the 2 ms (acoustic-ON) and sham conditions. **b.** Same as A, but for the 180 ms delay condition. **c.** SO-spindle event-event (left) and SO-SPWR event-event correlations (right) of acoustic-ON, time-locked to the SO trough. Horizontal lines correspond to significant differences between conditions (paired t-tests) for FDRs set to 0.05 (top line) and 0.01 (bottom line). Mean ± SEM for event-event coupling, mean for sham SO (grey line). Note, to facilitate comparisons with overlaid event-event correlations, the SO trough is depicted downward. Comparable figures for the other two delays are given in the **Supplementary Figure S4**.

correlations around the SO Down- to Up-State transition/Up-State (i.e., 100–200 ms after SO trough) for Up-state as compared to Down-state stimulation (see **Supplementary Figure S5** for comparisons between offline detected SOs in sham, acoustic-ON and acoustic-OFF, as well as for temporal distributions of acoustic-ON SO detections). The first part of NREM sleep during which ripples revealed increased density, amplitude RMS and duration (**Supplementary Table S4**) revealed closely similar SO-ripple event-event correlations (**Supplementary Figure S6**). On the other hand, neither ripple events coupled around spindles nor spindle events coupled around ripples revealed any significant modulation from sCLAS (**Supplementary Figure S7**).

4 | DISCUSSION

We aimed to investigate the hippocampal-thalamo-cortical interactions and the corresponding effect on a spatial memory task induced by acoustic stimulation delivered at different SO phases. We found that sCLAS affected behaviour dependent upon SO phase. Of the four sCLAS conditions, SO Up-state sCLAS, as expected (Moreira et al., 2021; Wunderlin et al., 2021), as well as Down-to-Up-state sCLAS revealed a preference index on the OPR task above chance, indicating successful memory for object location. Moreover, the preference index of Up-state sCLAS differed significantly from sCLAS at the late Up-state/Up-to-Down-state transition. Despite an apparent dependence of retention performance on the SO phase of acoustic stimulation, a significant effect relative to sham performance was not found. The lack of significance over sham was most likely due to our relatively short retention interval (as compared to rats, see e.g., Binder et al., 2012). We had selected a 3-h retention interval and had expected that in the sham condition animals would not perform above chance level since previously mice failed to reach above chance performance on the same task with retention intervals of 4-, 6-, and 24-hours (Murai et al., 2007). Previously, 2-h and shorter intervals had reported successful recent memory performance (Dere et al., 2005; Murai et al., 2007).

At the electrophysiological level, we first discuss the similarities and then differences between conditions which may be related to differential effects on retention. For all SO phases, sCLAS led to a sharp transient increment in ripples followed by a post-stimulus sustained suppression of thalamo-cortical spindle as well as hippocampal SPWR RMS and event-activity. Although the influence of a spindle refractory period has previously explained results of human EEG studies with acoustic stimulation (Antony et al., 2018; Ngo, Martinetz, et al., 2013; Weigenand et al., 2016) suppression of spindle activity in those studies was not as pronounced relative to the foregoing broad enhancement as observed here. A possible exception is the reduction of spike rates after epileptic seizures (Klinzing et al., 2021), which may be attributed to ion concentration dynamics (Krishnan & Bazhenov, 2011). Spindle termination is typically followed or leads to a refractory period attributed mostly to intrinsic currents activated during ongoing spindle activity in thalamic neurons. Indeed, one mechanism disclosed by in vitro studies involves an afterdepolarization generated by Ih current activation (Bal & McCormick, 1996; Fernandez & Lüthi, 2020). Yet, in vivo, corticothalamic activity is relevant for spindle synchronization (Contreras et al., 1997; Fernandez & Lüthi, 2020), and cortical desynchronization is also proposed as a possible mechanism for spindle termination (Bonjean et al., 2011). Sound and electric stimuli can induce cortical and thalamic activity (Dang-Vu et al., 2011; Sela et al., 2016), and produce spindle-like responses (Eckert et al., 2021; Vyazovskiy et al., 2009). The sustained post-stimulus spindle suppression is most easily interpreted as the result of intrinsic refractoriness subsequent to (short, 10 ms) acoustic stimulation, i.e., involving activation of specific ionic currents in a large neuronal population.

Hippocampal SPWR events are the result of excitatory-inhibitory network interactions with cessation dependent upon inhibitory currents (Howe et al., 2020; Malerba et al., 2016, 2019; Malerba & Bazhenov, 2019). Mechanisms are typically investigated on a shorter time scale (Buzsáki, 2015; McKenzie, 2018; Schlingloff et al., 2014) than could explain sustained ripple inhibition in our study. Yet recently, the fluorescent activity of post-SPWR inhibitory interneurons lasting up to about 2 seconds (Vancura et al., 2023) revealed results comparable to our study.

Importantly, event-related activity and stimulus-event correlation histogram both show an initial acute enhancement of mean hippocampal SPWR-activity, at all delays. Acoustic stimuli evoke not only brainstem but also hippocampal responses within 50 ms post-stimulation (Brankack & Buzsáki, 1986). Thus, we presume that strong depolarizing input of the acoustic stimulus, impacting the hippocampus in a state prone to generate ripples, can facilitate pyramidal cell-interneuron interactions producing increased ripple activity (Hu et al., 2023; Stark et al., 2014). The finding that cortical activity in the ripple range (Figure 3) is of lower magnitude than hippocampal ripples indicates that the transient increase in hippocampal ripples occurring shortly after onset of the acoustic stimulation is a direct physiological response to stimulation. Interestingly, the

transient increase in cortical ripples was followed by a sustained suppression in some conditions. Although again on a much shorter time scale, biological ripple events in cortex and hippocampus are associated (Khodagholy et al., 2017).

The main electrophysiological finding which distinguished Up-state sCLAS, for which retention performance was on average highest, was (for acoustic-ON) the coupling of ripples around SOs (Figure 5). Here, as compared to sham the temporal dynamics of SO-ripple coupling were more strongly modulated. This appears to mirror the typical occurrence of hippocampal and cortical ripples at the Down-to-Up-state transition/Up-state (Dickey et al., 2022; Khodagholy et al., 2017; Mölle et al., 2009; Figure 2b). The steeper drop compared to sham in SO-ripple coupling could be speculated as reflecting increased inhibitory tuning (McKenzie, 2018). Although SO-ripple coupling of Up-state sCLAS did reveal a significant difference over another sCLAS condition in which performance was not increased over chance level, the limited electrophysiological distinction over sham coincides with a non-significant difference in behaviour. This finding underscores the relevance of intact hippocampal activity during NREM sleep for memory retention on this spatial task and falls in line with recent experimental and modelling research revealing increasingly complex neurophysiological interdependencies between thalamo-cortical and hippocampal activity during NREM sleep (Azimi et al., 2021; Girardeau & Lopes-Dos-Santos, 2021; Sanda et al., 2021; Skelin et al., 2021; Wei et al., 2020). Moreover, our results support studies revealing that an unspecific facilitation of oscillatory coupling between brain structures associated putatively with reactivation, can facilitate memory consolidation (Campos-Beltran & Marshall, 2017; Maingret et al., 2016; Malkani & Zee, 2020). Successful unspecific reactivation may however require a relatively short interval between learning and interrogation putatively driving reactivation processes (Miyamoto et al., 2016), and is of low efficiency with the current procedure (e.g., Henin et al., 2019). It is also conceivable and would be of interest to investigate, whether specifically targeted memory activation reveals a higher efficiency with a longer time period between learning and manipulation periods. Furthermore, the effect of unspecifc stimuli in non-invasive brain stimulation procedures on memory consolidation in humans appears to rely strongly on the brain state, as either a trait or state property (Dehnavi et al., 2021; Krugliakova et al., 2022).

An unexpected finding was the difference in PreREM sleep duration which was significantly longer at SO-Up-state stimulation than for the behaviourally suboptimal sCLAS at the SO Up-to-Down-state transition. Time spent in all other sleep stages was the same at all sCLAS delays. It has been recently reported that spindle counts particularly during NREM/REM sleep transitions which would be scored as PreREM sleep in this study, is a good predictor of behavioural performance in mice during post-learning sleep (Yuan et al., 2021). Although we did not specifically count the density of spindle-like activity during this transition period, our results yield consistently, that PreREM sleep duration was longer at Up-state sCLAS than at the later stimulation at 300 ms delay. Although results did not uphold multiple comparisons testing NREM sleep spindle duration was also longer at the sCLAS Upstate than the Up-to-Down-state transition.

In summary, we showed that Down-state sCLAS can impair, and Up-state sCLAS may potentially enhance performance on a hippocampus-dependent OPR task in mice as reported for humans and rats (Moreira et al., 2021; Wunderlin et al., 2021). However, in contrast to those EEG studies, the presently measured electrophysiological activity responded less differently to CLAS, revealing only small differential responses for SO-ripple coupling. This paucity of electrophysiological and strong behavioural differences may reflect one limitation of our study, namely the small sample size, especially for two conditions. Moreover, SO detection in the above studies may have benefitted from a larger cortical representation instead of being obtained from a single LFP recording (Wunderlin et al., 2022). Finally, our experimental design may have benefitted from a longer minimal interstimulus interval. The fact that only pseudo-stimulation of SO Up-state at 180 ms (Figure 2b) was followed significantly by a more hyperpolarized potential level possibly indicates that the interval between acoustic and pseudo-stimulation (baseline level of pseudo-stimulation) was at a relatively more depolarized level than in the other conditions. To help understand how non-invasive stimulation procedures such as CLAS influence neural network activity and contribute to memory consolidation in sleep further rodent studies are warranted, with closely comparable stimulus designs to that in humans as well as studies specifically targeting task-relevant network activity, as e.g., hippocampo-cortical interactions in spatial or episodic tasks in rodents. Insight into neural brain responses and changes in inter-regional temporal dynamics to stimulation may, furthermore, facilitate understanding of the inter-individual differences in CLAS efficacy in humans.

AUTHOR CONTRIBUTIONS

Sonat Aksamaz: Data curation; formal analysis; writing—original draft. **Matthias Moelle:** Methodology; software; validation; writing—review and editing. **Esther Olubukola Akinola:** Formal analysis; writing—review and editing. **Erik Gromodka:** Formal analysis;

visualization. **Maxim Bazhenov:** Funding acquisition; writing—original draft. **Lisa Marshall:** Conceptualization; funding acquisition; methodology; project administration; resources; supervision; writing—original draft; writing—review and editing.

ACKNOWLEDGEMENTS

We gratefully thank Sonja Binder, Ana Martinez and Nasr Ghaleb for their technical support. This work was supported by the US-German Collaboration in Computational Neuroscience (NSF/BMBF grants 01GQ1706 and IIS-1724405), National Science Foundation (grant EFRI BRAID: 2223839), National Institutes of Health (grants 1RO1MH125557, 1R01NS109553, 1RO1MH117155 and 1R01NS104368). Open Access funding enabled and organized by Projekt DEAL.

CONFLICT OF INTEREST STATEMENT

The authors declare no conflicts of interest.

PEER REVIEW

The peer review history for this article is available at https://www.webofscience.com/api/gateway/wos/peer-review/10.1111/ejn.16116.

DATA AVAILABILITY STATEMENT

Data are available upon reasonable request.

ORCID

Lisa Marshall https://orcid.org/0000-0001-9118-3962

REFERENCES

Adamantidis, A. R., Gutierrez Herrera, C., & Gent, T. C. (2019). Oscillating circuitries in the sleeping brain. *Nature Reviews. Neuroscience*, *20*, 746–762. https://doi.org/10.1038/s41583-019-0223-4

Antony, J. W., Piloto, L., Wang, M., Pacheco, P., Norman, K. A., & Paller, K. A. (2018). Sleep spindle refractoriness segregates periods of memory reactivation. *Current Biology: CB*, *28*(11), 1736–1743.e4. https://doi.org/10.1016/j.cub.2018.04.020

Azimi, A., Alizadeh, Z., & Ghorbani, M. (2021). The essential role of hippocampo-cortical connections in temporal coordination of spindles and ripples. *NeuroImage*, *243*, 118485. https://doi.org/10.1016/j.neuroimage.2021.118485

Bal, T., & McCormick, D. A. (1996). What stops synchronized thalamocortical oscillations? *Neuron*, *17*, 297–308. https://doi.org/10.1016/S0896-6273(00)80161-0

Barker, G. R., & Warburton, E. C. (2011). When is the hippocampus involved in recognition memory? *The Journal of Neuroscience*, *31*, 10721–10731. https://doi.org/10.1523/JNEUROSCI.6413-10.2011

Benjamini, Y., & Hochberg, Y. (1995). Controlling the false discovery rate: A practical and powerful approach to multiple testing. *Journal of the Royal Statistical Society Series b-Methodological*, *57*, 289–300. https://doi.org/10.1111/j.2517-6161.1995.tb02031.x

Binder, S., Baier, P. C., Mölle, M., Inostroza, M., Born, J., & Marshall, L. (2012). Sleep enhances memory consolidation in the hippocampus-dependent object-place recognition task in rats. *Neurobiology of Learning and Memory*, *97*, 213–219. https://doi.org/10.1016/j.nlm.2011.12.004

Binder, S., Mölle, M., Lippert, M., Bruder, R., Aksamaz, S., Ohl, F., Wiegert, J. S., & Marshall, L. (2019). Monosynaptic hippocampal-prefrontal projections contribute to spatial memory consolidation in mice. *The Journal of Neuroscience*, *39*, 6978–6991. https://doi.org/10.1523/JNEUROSCI.2158-18.2019lisa.marshall@uni-luebeck.de

Bonjean, M., Baker, T., Lemieux, M., Timofeev, I., Sejnowski, T., & Bazhenov, M. (2011). Corticothalamic feedback controls sleep spindle duration in vivo. *The Journal of Neuroscience*, *31*, 9124–9134. https://doi.org/10.1523/JNEUROSCI.0077-11.2011

Brankack, J., & Buzsáki, G. (1986). Hippocampal responses evoked by tooth pulp and acoustic stimulation: Depth profiles and effect of behavior. *Brain Research*, *378*, 303–314. https://doi.org/10.1016/0006-8993(86)90933-9

Buzsáki, G. (1989). Two-stage model of memory trace formation: A role for "noisy" brain states. *Neuroscience*, *31*, 551–570. https://doi.org/10.1016/0306-4522(89)90423-5

Buzsáki, G. (2015). Hippocampal sharp wave-ripple: A cognitive biomarker for episodic memory and planning. *Hippocampus*, *25*, 1073–1188. https://doi.org/10.1002/hipo.22488

Campos-Beltran, D., & Marshall, L. (2017). Electric Stimulation to Improve Memory Consolidation During Sleep. In N. Axmacher & B. Rasch (Eds.), *Cognitive neuroscience of memory consolidation* (pp. 301–312). Springer.

Contreras, D., Destexhe, A., Sejnowski, T. J., & Steriade, M. (1997). Spatiotemporal patterns of spindle oscillations in cortex and thalamus. *The Journal of Neuroscience*, *17*, 1179–1196. https://doi.org/10.1523/JNEUROSCI.17-03-01179.1997

Cromwell, H. C., Mears, R. P., Wan, L., & Boutros, N. N. (2008). Sensory gating: A translational effort from basic to clinical science. *Clinical EEG and Neuroscience*, *39*, 69–72. https://doi.org/10.1177/155005940803900209

Dang-Vu, T. T., Bonjean, M., Schabus, M., Boly, M., Darsaud, A., Desseilles, M., Degueldre, C., Balteau, E., Phillips, C., Luxen, A., Sejnowski, T. J., & Maquet, P. (2011). Interplay between spontaneous and induced brain activity during human non-rapid eye movement sleep. *Proceedings of the National Academy of Sciences of the United States of America*, *108*, 15438–15443. https://doi.org/10.1073/pnas.1112503108

Dehnavi, F., Koo-Poeggel, P. C., Ghorbani, M., & Marshall, L. (2021). Spontaneous slow oscillation-slow spindle features predict induced overnight memory retention. *Sleep*, *44*, 1–12. https://doi.org/10.1093/sleep/zsab127

Dere, E., Huston, J. P., & De Souza Silva, M. A. (2005). Episodic-like memory in mice: Simultaneous assessment of object, place and temporal order memory. *Brain Research. Brain Research Protocols*, *16*, 10–19. https://doi.org/10.1016/j.brainresprot.2005.08.001

Dere, E., Huston, J. P., & De Souza Silva, M. A. (2007). The pharmacology, neuroanatomy and neurogenetics of one-trial object recognition in rodents. *Neuroscience and Biobehavioral*

Reviews, *31*, 673–704. https://doi.org/10.1016/j.neubiorev.2007.01.005

Dickey, C. W., Verzhbinsky, I. A., Jiang, X., Rosen, B. Q., Kajfez, S., Eskandar, E. N., Gonzalez-Martinez, J., Cash, S. S., & Halgren, E. (2022). Cortical ripples during NREM sleep and waking in humans. *The Journal of Neuroscience*, *42*, 7931–7946. https://doi.org/10.1523/JNEUROSCI.0742-22.2022

Diekelmann, S., & Born, J. (2010). The memory function of sleep. *Nature Reviews. Neuroscience*, *11*, 114–126. https://doi.org/10.1038/nrn2762

Eckert, M. J., Iyer, K., Euston, D. R., & Tatsuno, M. (2021). Reliable induction of sleep spindles with intracranial electrical pulse stimulation. *Learning & Memory (Cold Spring Harbor, N.Y.)*, *28*, 7–11. https://doi.org/10.1101/lm.052464.120

Ego-Stengel, V., & Wilson, M. A. (2010). Disruption of ripple-associated hippocampal activity during rest impairs spatial learning in the rat. *Hippocampus*, *20*, 1–10. https://doi.org/10.1002/hipo.20707

Fernandez, L. M. J., & Lüthi, A. (2020). Sleep spindles: Mechanisms and functions. *Physiological Reviews*, *100*, 805–868. https://doi.org/10.1152/physrev.00042.2018

Girardeau, G., Benchenane, K., Wiener, S. I., Buzsáki, G., & Zugaro, M. B. (2009). Selective suppression of hippocampal ripples impairs spatial memory. *Nature Neuroscience*, *12*, 1222–1223. https://doi.org/10.1038/nn.2384

Girardeau, G., & Lopes-Dos-Santos, V. (2021). Brain neural patterns and the memory function of sleep. *Science*, *374*, 560–564. https://doi.org/10.1126/science.abi8370

Glin, L., Arnaud, C., Berracochea, D., Galey, D., Jaffard, R., & Gottesmann, C. (1991). The intermediate stage of sleep in mice. *Physiology & Behavior*, *50*, 951–953. https://doi.org/10.1016/0031-9384(91)90420-S

Henin, S., Borges, H., Shankar, A., Sarac, C., Melloni, L., Friedman, D., Flinker, A., Parra, L. C., Buzsaki, G., Devinsky, O., & Liu, A. (2019). Closed-loop acoustic stimulation enhances sleep oscillations but not memory performance. *Eneuro*, *6*, ENEURO.0306-0319. https://doi.org/10.1523/ENEURO.0306-19.2019

Howe, T., Blockeel, A. J., Taylor, H., Jones, M. W., Bazhenov, M., & Malerba, P. (2020). NMDA receptors promote hippocampal sharp-wave ripples and the associated coactivity of CA1 pyramidal cells. *Hippocampus*, *30*, 1356–1370. https://doi.org/10.1002/hipo.23276

Hu, H., Hostetler, R. E., & Agmon, A. (2023). Ultrafast (400 Hz) network oscillations induced in mouse barrel cortex by optogenetic activation of thalamocortical axons. *eLife*, *12*, 1–29. https://doi.org/10.7554/eLife.82412

Ketz, N., Jones, A. P., Bryant, N. B., Clark, V. P., & Pilly, P. K. (2018). Closed-loop slow-wave tACS improves sleep-dependent long-term memory generalization by modulating endogenous oscillations. *The Journal of Neuroscience*, *38*, 7314–7326. https://doi.org/10.1523/JNEUROSCI.0273-18.2018

Khodagholy, D., Gelinas, J. N., & Buzsáki, G. (2017). Learning-enhanced coupling between ripple oscillations in association cortices and hippocampus. *Science*, *358*, 369–372. https://doi.org/10.1126/science.aan6203

Klinzing, J. G., Niethard, N., & Born, J. (2019). Mechanisms of systems memory consolidation during sleep. *Nature Neuroscience*, *22*, 1598–1610. https://doi.org/10.1038/s41593-019-0467-3

Klinzing, J. G., Tashiro, L., Ruf, S., Wolff, M., Born, J., & Ngo, H. V. (2021). Auditory stimulation during sleep suppresses spike activity in benign epilepsy with centrotemporal spikes. *Cell Reports Medicine*, *2*, 100432. https://doi.org/10.1016/j.xcrm.2021.100432

Koo-Poeggel, P., Neuwerk, S., Petersen, E., Grasshoff, J., Mölle, M., Martinetz, T., & Marshall, L. (2022). Closed-loop acoustic stimulation during an afternoon nap to modulate subsequent encoding. *Journal of Sleep Research*, *31*, e13734. https://doi.org/10.1111/jsr.13734

Krishnan, G. P., & Bazhenov, M. (2011). Ionic dynamics mediate spontaneous termination of seizures and postictal depression state. *The Journal of Neuroscience*, *31*, 8870–8882. https://doi.org/10.1523/JNEUROSCI.6200-10.2011

Krugliakova, E., Skorucak, J., Sousouri, G., Leach, S., Snipes, S., Ferster, M. L., Da Poian, G., Karlen, W., & Huber, R. (2022). Boosting recovery during sleep by means of auditory stimulation. *Frontiers in Neuroscience*, *16*, 755958. https://doi.org/10.3389/fnins.2022.755958

Ladenbauer, J., Ladenbauer, J., Külzow, N., & Flöel, A. (2021). Memory-relevant nap sleep physiology in healthy and pathological aging. *Sleep*, *44*, 1–13. https://doi.org/10.1093/sleep/zsab002

Maingret, N., Girardeau, G., Todorova, R., Goutierre, M., & Zugaro, M. (2016). Hippocampo-cortical coupling mediates memory consolidation during sleep. *Nature Neuroscience*, *19*, 959–964. https://doi.org/10.1038/nn.4304

Malerba, P., & Bazhenov, M. (2019). Circuit mechanisms of hippocampal reactivation during sleep. *Neurobiology of Learning and Memory*, *160*, 98–107. https://doi.org/10.1016/j.nlm.2018.04.018

Malerba, P., Krishnan, G. P., Fellous, J. M., & Bazhenov, M. (2016). Hippocampal CA1 ripples as inhibitory transients. *PLoS Computational Biology*, *12*, e1004880. https://doi.org/10.1371/journal.pcbi.1004880

Malerba, P., Rulkov, N. F., & Bazhenov, M. (2019). Large time step discrete-time modeling of sharp wave activity in hippocampal area CA3. *Communications in Nonlinear Science and Numerical Simulation*, *72*, 162–175. https://doi.org/10.1016/j.cnsns.2018.12.009

Malkani, R. G., & Zee, P. C. (2020). Brain stimulation for improving sleep and memory. *Sleep Medicine Clinics*, *15*, 101–115. https://doi.org/10.1016/j.jsmc.2019.11.002

Marshall, L., Cross, N., Binder, S., & Dang-Vu, T. T. (2020). Brain rhythms during sleep and memory consolidation: Neurobiological insights. *Physiology (Bethesda, Md.)*, *35*, 4–15. https://doi.org/10.1152/physiol.00004.2019

Marshall, L., Helgadóttir, H., Mölle, M., & Born, J. (2006). Boosting slow oscillations during sleep potentiates memory. *Nature*, *444*, 610–613. https://doi.org/10.1038/nature05278

McKenzie, S. (2018). Inhibition shapes the organization of hippocampal representations. *Hippocampus*, *28*, 659–671. https://doi.org/10.1002/hipo.22803

Miyamoto, D., Hirai, D., Fung, C. C., Inutsuka, A., Odagawa, M., Suzuki, T., Boehringer, R., Adaikkan, C., Matsubara, C., Matsuki, N., Fukai, T., McHugh, T. J., Yamanaka, A., & Murayama, M. (2016). Top-down cortical input during NREM sleep consolidates perceptual memory. *Science*, *352*, 1315–1318. https://doi.org/10.1126/science.aaf0902

Mölle, M., Eschenko, O., Gais, S., Sara, S. J., & Born, J. (2009). The influence of learning on sleep slow oscillations and associated spindles and ripples in humans and rats. *The European Journal of Neuroscience*, *29*, 1071–1081. https://doi.org/10.1111/j.1460-9568.2009.06654.x

Moreira, C. G., Baumann, C. R., Scandella, M., Nemirovsky, S. I., Leach, S., Huber, R., & Noain, D. (2021). Closed-loop auditory stimulation method to modulate sleep slow waves and motor learning performance in rats. *eLife*, *10*, 1–23. https://doi.org/10.7554/eLife.68043

Mumby, D. G., Gaskin, S., Glenn, M. J., Schramek, T. E., & Lehmann, H. (2002). Hippocampal damage and exploratory preferences in rats: Memory for objects, places, and contexts. *Learning & Memory*, *9*, 49–57. https://doi.org/10.1101/lm.41302

Murai, T., Okuda, S., Tanaka, T., & Ohta, H. (2007). Characteristics of object location memory in mice: Behavioral and pharmacological studies. *Physiology & Behavior*, *90*, 116–124. https://doi.org/10.1016/j.physbeh.2006.09.013

Ngo, H. V., Claussen, J. C., Born, J., & Mölle, M. (2013). Induction of slow oscillations by rhythmic acoustic stimulation. *Journal of Sleep Research*, *22*, 22–31. https://doi.org/10.1111/j.1365-2869.2012.01039.x

Ngo, H. V., Martinetz, T., Born, J., & Mölle, M. (2013). Auditory closed-loop stimulation of the sleep slow oscillation enhances memory. *Neuron*, *78*, 545–553. https://doi.org/10.1016/j.neuron.2013.03.006

Ngo, H. V., Miedema, A., Faude, I., Martinetz, T., Mölle, M., & Born, J. (2015). Driving sleep slow oscillations by auditory closed-loop stimulation-a self-limiting process. *The Journal of Neuroscience*, *35*, 6630–6638. https://doi.org/10.1523/JNEUROSCI.3133-14.2015

Novitskaya, Y., Sara, S. J., Logothetis, N. K., & Eschenko, O. (2016). Ripple-triggered stimulation of the locus coeruleus during post-learning sleep disrupts ripple/spindle coupling and impairs memory consolidation. *Learning & Memory*, *23*, 238–248. https://doi.org/10.1101/lm.040923.115

Ong, J. L., Lau, T. Y., Lee, X. K., van Rijn, E., & Chee, M. W. L. (2020). A daytime nap restores hippocampal function and improves declarative learning. *Sleep*, *43*, 1–9. https://doi.org/10.1093/sleep/zsaa058

Ong, J. L., Lo, J. C., Chee, N. I., Santostasi, G., Paller, K. A., Zee, P. C., & Chee, M. W. (2016). Effects of phase-locked acoustic stimulation during a nap on EEG spectra and declarative memory consolidation. *Sleep Medicine*, *20*, 88–97. https://doi.org/10.1016/j.sleep.2015.10.016

Oudiette, D., Antony, J. W., Creery, J. D., & Paller, K. A. (2013). The role of memory reactivation during wakefulness and sleep in determining which memories endure. *The Journal of Neuroscience*, *33*, 6672–6678. https://doi.org/10.1523/JNEUROSCI.5497-12.2013

Rasch, B., & Born, J. (2013). About sleep's role in memory. *Physiological Reviews*, *93*, 681–766. https://doi.org/10.1152/physrev.00032.2012

Salfi, F., D'Atri, A., Tempesta, D., De Gennaro, L., & Ferrara, M. (2020). Boosting slow oscillations during sleep to improve memory function in elderly people: A review of the literature. *Brain Sciences*, *10*, 300. https://doi.org/10.3390/brainsci10050300

Sanda, P., Malerba, P., Jiang, X., Krishnan, G. P., Gonzalez-Martinez, J., Halgren, E., & Bazhenov, M. (2021). Bidirectional interaction of hippocampal ripples and cortical slow waves leads to coordinated spiking activity during NREM sleep. *Cerebral Cortex (New York, N.Y.: 1991)*, *31*, 324–340.

Schlingloff, D., Káli, S., Freund, T. F., Hájos, N., & Gulyás, A. I. (2014). Mechanisms of sharp wave initiation and ripple generation. *The Journal of Neuroscience*, *34*, 11385–11398. https://doi.org/10.1523/JNEUROSCI.0867-14.2014

Sela, Y., Vyazovskiy, V. V., Cirelli, C., Tononi, G., & Nir, Y. (2016). Responses in rat Core auditory cortex are preserved during sleep spindle oscillations. *Sleep*, *39*, 1069–1082. https://doi.org/10.5665/sleep.5758

Skelin, I., Zhang, H., Zheng, J., Ma, S., Mander, B. A., Kim McManus, O., Vadera, S., Knight, R. T., McNaughton, B. L., & Lin, J. J. (2021). Coupling between slow waves and sharp-wave ripples engages distributed neural activity during sleep in humans. *Proceedings of the National Academy of Sciences of the United States of America*, *118*, 118. https://doi.org/10.1073/pnas.2012075118

Stark, E., Roux, L., Eichler, R., Senzai, Y., Royer, S., & Buzsáki, G. (2014). Pyramidal cell-interneuron interactions underlie hippocampal ripple oscillations. *Neuron*, *83*, 467–480. https://doi.org/10.1016/j.neuron.2014.06.023

Süer, C., Dolu, N., & Ozesmi, C. (2004). The effect of immobilization stress on sensory gating in mice. *The International Journal of Neuroscience*, *114*, 55–65. https://doi.org/10.1080/00207450490249400

Swift, K. M., Gross, B. A., Frazer, M. A., Bauer, D. S., Clark, K. J. D., Vazey, E. M., Aston-Jones, G., Li, Y., Pickering, A. E., Sara, S. J., & Poe, G. R. (2018). Abnormal locus Coeruleus sleep activity alters sleep signatures of memory consolidation and impairs place cell stability and spatial memory. *Current Biology*, *28*, 3599–3609.e3594. https://doi.org/10.1016/j.cub.2018.09.054

Tonegawa, S., Morrissey, M. D., & Kitamura, T. (2018). The role of engram cells in the systems consolidation of memory. *Nature Reviews. Neuroscience*, *19*, 485–498. https://doi.org/10.1038/s41583-018-0031-2

Vancura, B., Geiller, T., Grosmark, A., Zhao, V., & Losonczy, A. (2023). Inhibitory control of sharp-wave ripple duration during learning in hippocampal recurrent networks. *Nature Neuroscience*, *26*, 788–797. https://doi.org/10.1038/s41593-023-01306-7

Vyazovskiy, V. V., Faraguna, U., Cirelli, C., & Tononi, G. (2009). Triggering slow waves during NREM sleep in the rat by intracortical electrical stimulation: Effects of sleep/wake history and background activity. *Journal of Neurophysiology*, *101*, 1921–1931. https://doi.org/10.1152/jn.91157.2008

Wei, Y., Krishnan, G. P., Marshall, L., Martinetz, T., & Bazhenov, M. (2020). Stimulation augments spike sequence replay and memory consolidation during slow-wave sleep. *The Journal of Neuroscience*, *40*, 811–824. https://doi.org/10.1523/JNEUROSCI.1427-19.2019

Weigenand, A., Mölle, M., Werner, F., Martinetz, T., & Marshall, L. (2016). Timing matters: Open-loop stimulation does not improve overnight consolidation of word pairs in humans. *The European Journal of Neuroscience*, *44*, 2357–2368. https://doi.org/10.1111/ejn.13334

Witten, L., Bastlund, J. F., Glenthøj, B. Y., Bundgaard, C., Steiniger-Brach, B., Mørk, A., & Oranje, B. (2016). Comparing

pharmacological modulation of sensory gating in healthy humans and rats: The effects of Reboxetine and haloperidol. *Neuropsychopharmacology: Official Publication of the American College of Neuropsychopharmacology*, *41*, 638–645. https://doi.org/10.1038/npp.2015.194

Wunderlin, M., Koenig, T., Zeller, C., Nissen, C., & Züst, M. A. (2022). Automatized online prediction of slow-wave peaks during non-rapid eye movement sleep in young and old individuals: Why we should not always rely on amplitude thresholds. *Journal of Sleep Research*, *31*, e13584. https://doi.org/10.1111/jsr.13584

Wunderlin, M., Züst, M. A., Hertenstein, E., Fehér, K. D., Schneider, C. L., Klöppel, S., & Nissen, C. (2021). Modulating overnight memory consolidation by acoustic stimulation during slow-wave sleep: A systematic review and meta-analysis. *Sleep*, *44*, 1–11. https://doi.org/10.1093/sleep/zsaa296

Yuan, R. K., Lopez, M. R., Ramos-Alvarez, M.-M., Normandin, M. E., Thomas, A. S., Uygun, D. S., Cerda, V. R., Grenier, A. E., Wood, M. T., Gagliardi, C. M., Guajardo, H., & Muzzio, I. A. (2021). Differential effect of sleep deprivation on place cell representations, sleep architecture, and memory in young and old mice. *Cell Reports*, *35*, 109234. https://doi.org/10.1016/j.celrep.2021.109234

SUPPORTING INFORMATION

Additional supporting information can be found online in the Supporting Information section at the end of this article.

How to cite this article: Aksamaz, S., Mölle, M., Akinola, E. O., Gromodka, E., Bazhenov, M., & Marshall, L. (2023). Single closed-loop acoustic stimulation targeting memory consolidation suppressed hippocampal ripple and thalamo-cortical spindle activity in mice. *European Journal of Neuroscience*, 1–18. https://doi.org/10.1111/ejn.16116